ARTICLE

Novel ruthenium complexes bearing bipyridine-based and *N*-heterocyclic carbene-supported pyridine (NCN) ligands: the influence of ligands for catalytic transfer hydrogenation of ketones

Received 00th January 20xx,
Accepted 00th January 20xx

DOI: 10.1039/x0xx00000x

Akkharadet Piyasaengthong,*[a,b] Luke J. Williams,[a] Dmitry S. Yufit[a] and James W. Walton *[a]

Transfer hydrogenation (TH) is a powerful synthetic tool in the production of secondary alcohols from ketones by using a non-H_2 hydrogen source along with metal catalysts. Among homogeneous catalysts, Ru(II) complexes are the most efficient catalysts. In our research, six novel ruthenium(II) complexes bearing bipyridine-based ligands, [Ru(**L1**)Cl_2] (**1**), [Ru(**L1**)(PPh_3)Cl]Cl (**2**) and [Ru(**L2**)Cl_2] (**3**) and *N*-heterocyclic carbene-supported pyridine (NCN) ligand, [RuCp(**L3**)]PF_6 (**4**), [RuCp*(**L3**)]PF_6 (**5**), and [Ru(*p*-cymene)(**L3**)Cl]PF_6 (**6**) (where, **L1** = 6,6′-Bis(aminomethyl)-2,2′-bipyridine, **L2** = 6,6′-bis(dimethylaminomethyl)-2,2′-bipyridine and **L3** = 1,3-bis(2-methylpyridyl)imidazolium bromide) were synthesised and characterised by NMR spectroscopy, HRMS, and X-ray crystallography. The catalytic transfer hydrogenation of 27 ketones in 2-propanol at 80 °C in the presence of KO*t*Bu (5 mol%) was demonstrated and the effect of ligands is highlighted. The results show that catalyst **1** exhibits improved TH efficiency compared to the commercially available Milstein catalyst and displays higher catalytic activity than **2** due to the steric effect from PPh_3. In combination between kinetic data and Eyring analysis, an observed zero-order dependence of the acetophenone substrate implies a rate-limiting hydride transfer step, leading to proposed an inner-sphere hydride transfer mechanism.

Introduction

Transfer hydrogenation (TH) is a powerful synthetic tool in the production of secondary alcohols from ketones, which uses a non-H_2 gas source of hydrogen along with a metal catalyst.[1] Among various transition metals catalysts used in this reaction, such as Fe,[2,3] Ru,[4,5] Os,[6] Co,[7,8] Rh,[9] Ir,[10] Ni,[11] Pd,[12] and Au,[13] Ru(II) complexes are one of the most efficient class of catalysts.[14,15]

The effect of the ligands in the Ru(II) complexes plays a crucial role toward both selectivity and activity of the catalyst.[1] Following the successful of 1,2-diamines in Noyori-type catalysts for TH of carbonyl compounds,[16] Ru(II) complexes bearing alternative *N*-based donor ligands have been investigated for their catalytic activities.[17] Ru catalysts with bipyridine (bpy) were studied for TH in water, giving high conversions (97%) for a range of aromatic ketones into their corresponding alcohols.[18] Many examples of successful Ru catalysts for the hydrogenolysis of carbonyl groups have been reported, containing bpy, BINAP and diamine ligands, amongst others.[19,20]

N-heterocyclic carbene (NHC) ligands are commonly found in the development of metal catalysts. With respect to hydrogenation catalysts, the strong σ-donating ability of the carbene carbon enhances the nucleophilicity of the Ru–hydride catalytic intermediate and variation in the two adjacent σ-withdrawing and π-donating nitrogen atom substituents leads to variation in the electronic and steric stabilization of the complex.[21–24] Ru-NHC complexes have been applied in TH of substituted aromatic ketones giving good to excellent yields.[25–27] Of particular note, Ru pincer complexes bearing pyridyl-supported NHC ligands exhibited high catalytic activity, giving TONs and TOFs of up to 126,000 and 15,200 h^{-1}, respectively.[28]

Following the success of Ru catalysts containing bpy and NHC ligands, herein we report two families of novel Ru catalysts with bipyridine-based ligands (**1**-**3**) and with NHC-supported pyridine (NCN) ligands (**4**-**6**), as shown in Scheme 1. The synthesis and characterisation of these complexes are reported, followed by their catalytic activities in the TH of ketones. High activity is seen for several complexes and mechanistic investigation leads to a proposed inner-sphere mechanism.

[a] *Department of Chemistry, Durham University, South Road, Durham, DH1 3LE, United Kingdom*
[b] *Bioscience program, Faculty of Science, Kasetsart University, Chatuchak, Bangkok 10900, Thailand*
[c] **correspondence to p.akkharadet@gmail.com*

† Electronic Supplementary Information (ESI) available: NMR and mass spectra and information on X-ray crystal structure. CCDC 2099625-2099628. For ESI and crystallographic data in CIF or other electronic format see DOI: 10.1039/x0xx00000x

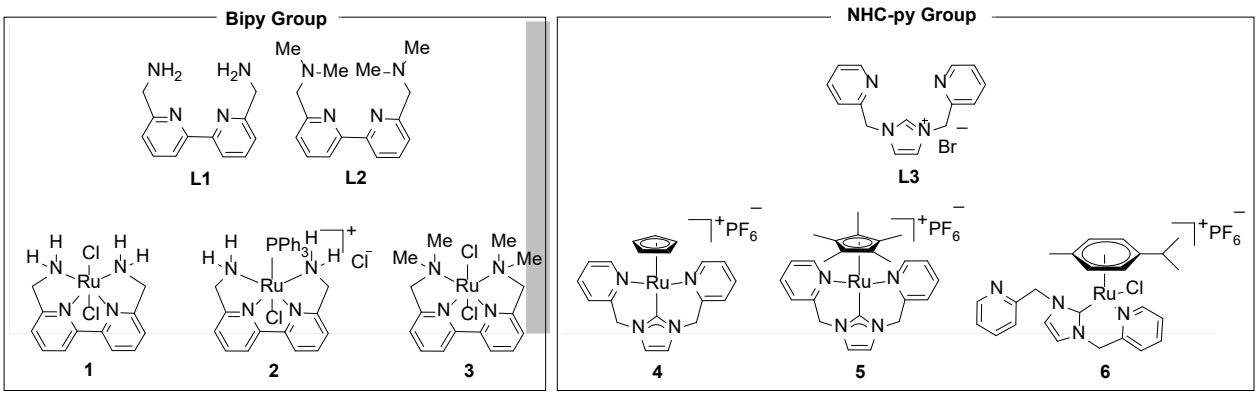

Scheme 1 Ligands (**L1**–**L3**) and novel Ru complexes (**1**-**6**).

Results and discussion

Synthesis and characterisation

Ligands **L1** and **L2** were prepared through modification of literature procedures, as shown in Scheme 2.[29] Heating 6,6'-dimethyl-2,2'-bipyridine with *N*-bromosuccinimide along with catalytic benzoyl peroxide afforded **L0**. Careful control over stoichiometries allowed for high yields of dibrominated **L0**, which was purified by recrystalisation. **L0** was then reacted with hexamethylenetetramine or dimethylamine to generate **L1** and **L2**, respectively. The Ru catalysts **1** and **3** were obtained by the reaction of $[RuCl_2(p\text{-cymene})]_2$ with **L1** and **L2**, respectively, under a N_2 inert atmosphere. **L1** reacted with $RuCl_2(PPh_3)_3$ to afford catalyst **2**, in which one PPh_3 ligand remains within the complex. Interestingly, only catalyst **2** was stable when exposed to air at ambient temperature, while catalysts **1** and **3** were air and moisture sensitive solids.

Ligand **L3** was synthesised according to O'Hearn and Singer.[30] Novel Ru catalysts **4**-**6** were obtained from the reaction between **L3** and Ag_2O to generate a Ag-NHC complex, before transmetallation with $[CpRu(MeCN)_3]PF_6$, $[Cp^*Ru(MeCN)_3]PF_6$ and $[RuCl_2(p\text{-cymene})]_2$, gave complexes **4**, **5** and **6**, respectively (Scheme 3). Interestingly, while **L3** acts as a tridentate ligand Cp-derived complexes **4** and **5**, in complex **6**, ligand **L3** is bidentate, presumably due to steric constraints due to the *p*-cymene ligand.

The NMR and HRMS spectra of **1**-**6** confirmed complex formation between Ru and **L1**-**L3**, as detailed in the supplementary information. It is worth noting that in complex **2** the two methylene protons are diastereotopic, giving doublets ($^2J_{HH}$ = 17.5), due to the spatial arrangement of the two protons, with one pointing towards the PPh_3 group and the other towards the chloride ligand. The $^{31}P\{^1H\}$ NMR spectrum of catalyst **2** reveal a singlet at 58.5 ppm, indicating only one phosphorus environment. Single crystals of **2** were grown by slow evaporation in MeOH and X-ray crystallography (Fig. 1a) confirming a single PPh_3 ligand bound to the Ru centre. Recrystallization of catalyst **5** in DCM:EtOH (1:1) by slow evaporation also led to formation of single crystals, suitable for X-ray crystallography (Fig. 1b).

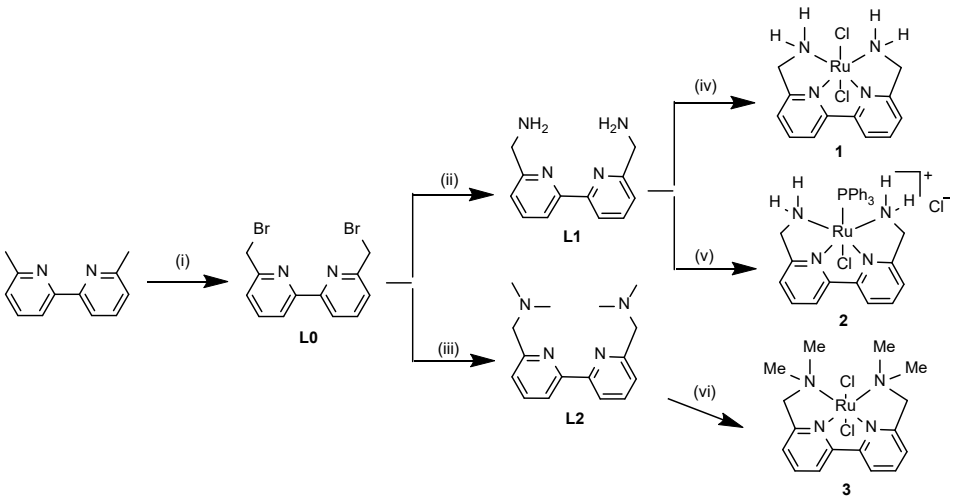

Scheme 2 Synthesis of ligands **L1-L2** and complexes **1–3**. Conditions: (i) NBS, DBPO, $CHCl_3$, 62 °C, 16 h; (ii) $(CH_2)_6N_4$, $CHCl_3$, 62 °C, 4 h; (iii) $(CH_3)_2NH$, EtOH, 80 °C, 16 h; (iv) $[RuCl_2(p\text{-cymene})]_2$, N_2, DCM, rt, 1 h; (v) $RuCl_2(PPh_3)_3$, N_2, $CHCl_3$, 62 °C, 14 h; (vi) $[RuCl_2(p\text{-cymene})]_2$, N_2, DCM, 50 °C, 16 h;

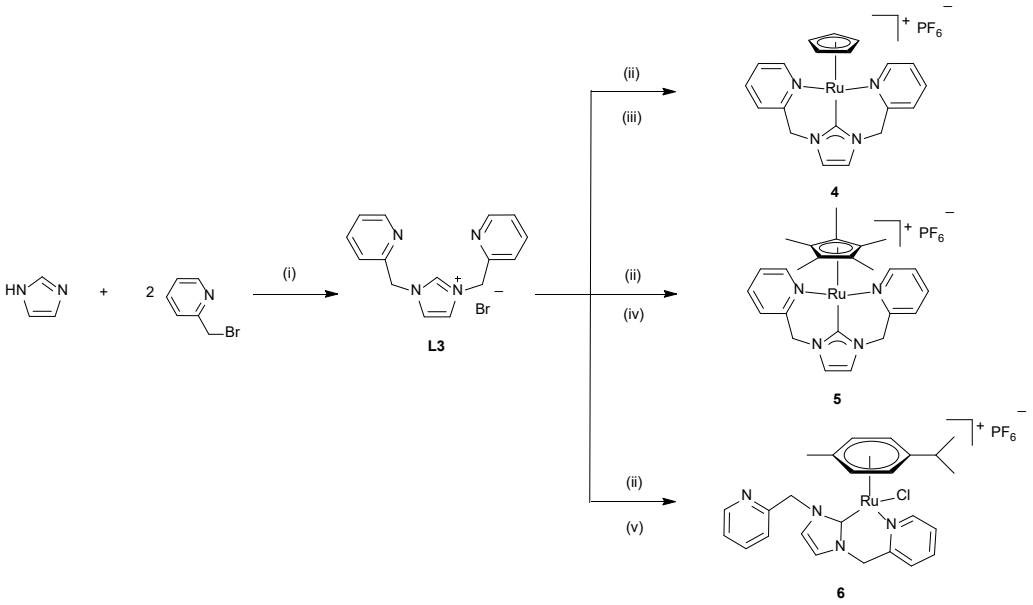

Scheme 3 Synthesis of ligands **L3** and complexes **4**–**6**. Conditions: (i) K_2CO_3, MeOH, 66 °C, 48 h; (ii) Ag_2O, EtOH:DCM (1:1), N_2, rt, 1.5 h, dark; (iii) $[CpRu(MeCN)_3]PF_6$, N_2, 50 °C, 16 h, dark; (iv) $[Cp^*Ru(MeCN)_3]PF_6$, N_2, 50 °C, 16 h, dark; (v) $[RuCl_2(p\text{-cymene})]_2$, N_2, 70 °C, 16 h, dark, $AgPF_6$;

X-ray crystal structures

Crystal and molecular structures of complexes **2** and **5** (Fig. 1), as well as those of precursor **L0** (S43) and the free ligand, **L1** (crystallised as a tri-hydrochloride salt monohydrate, Fig. S44), were determined by single crystal X-ray crystallography and confirmed the expected structures. Heterocycles in both **L0** and **L1** are coplanar, however the conformation of the molecule is *s-trans* in **L0** (the molecule is located in the centre of symmetry) and *s-cis* in **L1.** This is another illustration of conformational flexibility of bipyridine derivatives. Molecules **L1** in the crystal structure are arranged in anti-parallel stacks, linked by numerous N/O-H...Cl hydrogen bonds, while the packing of molecules **L0** is determined by Br...Br interactions. Some aromatic fragments of adjacent molecules in structure **L0** are also parallel but there is almost no overlapping between them and therefore any contribution of π...π interactions should be negligible.

The Ru atom in complex **2** adopts nearly ideal tetragonal bi-pyramidal coordination. The *trans* arrangement of Cl and PPh_3 is confirmed with the 4 N donors forming a square plane arrangement. The tetra-dentate ligand occupying all equatorial coordinating positions is non-planar, likely due to steric repulsion from the large PPh_3 ligand. In the crystal structure, complex **2** forms double layers with PPh_3 ligands directed outwards. The molecules in layers are linked by various hydrogen bonds, inter-connecting cations, anions and solvent (water and methanol) molecules (Fig. S45).

The coordination mode of the Ru-atom in complex **5** can be described as a "3-legged piano stool" and the tri-dentate ligand is significantly non-planar. The Ru centre has d^{18} electronic configuration and is coordinatively saturated, with no labile ligands. No hydrogen bonds are present in structure **5** and the molecules are linked there by π...π interactions and weak C-H...F contacts (Fig. S46). This differences in the Ru coordination mode across the series is likely a reason for the different catalytic properties of the complexes.

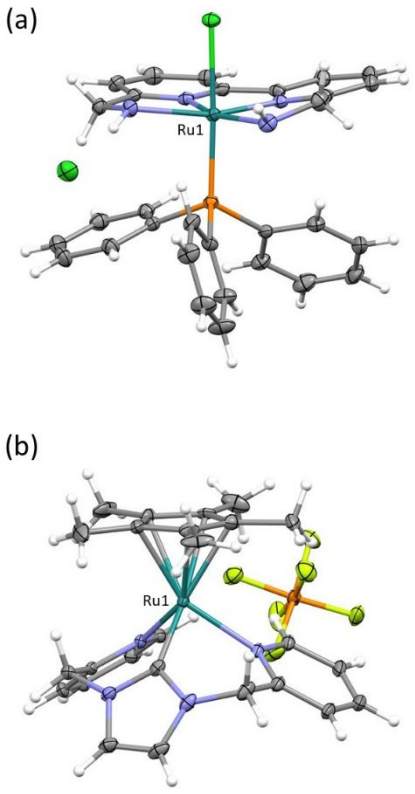

Fig. 1 Molecular structures of Ru complexes (a) **2** and (b) **5** with thermal ellipsoids shown at 50% and 20% probability, respectively. Solvent molecules outside the coordination sphere are omitted for clarity.

Transfer Hydrogenation Optimisation

Catalyst **1** was used as a representative catalyst and the TH of acetophenone to 1-phenylethanol in 2-propanol solvent was optimised through variation in base, temperature, reaction time and catalyst concentration (Table 1). Almost quantitative conversion (97%) was observed within 10 min at 100 °C (TOF 582 h^{-1}), using KO*t*Bu (5 mol %) base and 1 mol % of Ru catalyst **1** (entry 1). At 90 °C, the reaction still proceeds to almost quantitative yield (>99%), but requires a longer reaction time of 30 min (entry 2). Reducing the temperature further to 80 °C gave excellent catalytic activity (>99%) within 1 h (entry 3). Further reduction in reaction temperature led to lower conversions and no reaction was observed at 20 °C (entry 6). Variation in the base and base concentration were also tested. Over a period of 30 min, product formation was observed at 99%, 92% and 86% in the presence of KO*t*Bu at 10, 5 and 2.5 mol%, respectively (entry 3, 7 and 8), while there was no product in the absence of base (entry 20). KO*t*Bu displays higher TH efficiency, compared to NaO*t*Bu (entry 3 and 9), which is likely due to the observed low solubility of NaO*t*Bu in the reaction mixture. KOH and NaOH showed low and equivalent activity (entry 10 and 11), which may imply that the alkali-metal cation is not directly involved in the rate-determining step of the reaction mechanism. While there is a report referring to the effect of the alkali-metal cations within the base on the rate of TH,[31] no significant difference is observed here between KOH and NaOH, which is consistent with similar Ru-*NNN* complexes published by Chen and Wang.[32,33] A selection of other bases showed much poorer performance (entries 12-16). Varying the amount of catalyst from 0.5 mol % to 5 mol % revealed that catalyst efficiency peaked at 1 mol % catalyst, before dropping dramatically at 5 mol % (entries 17-19). It is not clear why the efficiency drops at high catalyst loading, but this could be attributed to low solubility and catalyst precipitation.

Table 1 Optimizing of reaction conditions for catalytic transfer hydrogenation of acetophenone in 2-propanol.

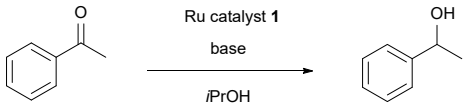

Entry	Cat.	Base	Ketone/base/cat. (mol %)	Temp. (°C)	Conv. (%)[a] 10 min	30 min	60 min
1	**1**	KO*t*Bu	100/5/1	100	97	>99	>99
2	**1**	KO*t*Bu	100/5/1	90	63	>99	>99
3	**1**	KO*t*Bu	100/5/1	80	63	92	>99 (69)[b]
4	**1**	KO*t*Bu	100/5/1	60	6	15	34
5	**1**	KO*t*Bu	100/5/1	40	0	3	6
6	**1**	KO*t*Bu	100/5/1	20	0	0	0
7	**1**	KO*t*Bu	100/10/1	80	63	99	>99
8	**1**	KO*t*Bu	100/2.5/1	80	55	86	97
9	**1**	NaO*t*Bu	100/5/1	80	25	66	96
10	**1**	KOH	100/5/1	80	31	82	96
11	**1**	NaOH	100/5/1	80	32	84	>99
12	**1**	NaH	100/5/1	80	10	25	46
13	**1**	DMAP	100/5/1	80	0	0	0
14	**1**	K_2CO_3	100/5/1	80	0	1	4
15	**1**	DBU	100/5/1	80	0	0	0
16	**1**	DBN	100/5/1	80	0	0	0
17	**1**	KO*t*Bu	100/5/0.5	80	1	6	10
18	**1**	KO*t*Bu	100/5/2.5	80	35	82	>99
19	**1**	KO*t*Bu	100/5/5	80	10	17	25
20	**1**	-	100/0/1	80	0	0	0

Reaction conditions: acetophenone (0.5 mmol), base, Ru catalyst, and 2-propanol (2.5 mL). [a]Determined by ^{1}H NMR spectroscopy using dimethyl sulfoxide as internal standard, [b]data in parentheses refers to yields of isolated products.

Catalytic Activity of Complexes 1-6 in transfer hydrogenation of acetophenone

Novel Ru catalysts **1**-**6** (1 mol %) were tested for TH of acetophenone under the reaction condition in 2-propanol at 80 °C in the presence of KO*t*Bu (5 mol %). Activity was compared to the commercially available Ru-MACHO and Milstein catalyst (see Fig S58 for catalyst structures), as shown in Table 2.

Ru catalysts with bipyridine-based ligands **1** and **2** displayed excellent catalytic activities, giving the same percent conversion of 92% within 30 min (entry 1-2). This represents improved TH efficiency compared to the Milstein catalyst (entry 7), although their catalytic performances were lower than Ru-MACHO (entry 8), which was able to convert acetophenone to the corresponding alcohol up to 97% conversion at room temperature (supporting information). Catalyst **3** showed moderate catalytic activity, reaching almost quantitative conversion within 16 h.

Unfortunately, low catalytic activities were observed for Ru catalysts bearing NHC-pyridine (NCN) ligands **4**-**6** (entry 4-6). In the case of catalyst **4**-**5**, low activity is attributed to the steric effect of the pyridines and a lack of coordination between the Ru centre and the substrate, due to the strong coordinate bond between Ru and the nitrogen atoms in the pyridine ligands, hindering substrate coordination. For catalyst **6**, a labile chloride ligand provides a potential site for substrate to bind, however, low activity was also observed, potentially due to the steric effects of the *p*-cymene.

Table 2 Catalytic activity of complexes **1**-**6** in TH of acetophenone.

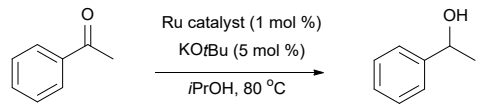

Entry	Cat.	Conv. (%)[a]				
		10 min	30 min	60 min	180 min	960 min
1	**1**	63	92	>99	>99	>99
2	**2**	73	92	>99	>99	>99
3	**3**	14	20	51	84	>99
4	**4**	0	1	6	7	18
5	**5**	0	1	1	4	24
6	**6**	0	1	1	3	15
7	Milstein catalyst	38	63	79	>99	>99
8	Ru-MACHO	>99	>99	>99	>99	>99

Reaction conditions: acetophenone (0.5 mmol), KO*t*Bu (0.025 mmol, 5 mol %), Ru catalyst (0.005 mmol, 1 mol %), and 2-propanol (2.5 mL) at 80 °C. [a]Determined by ^{1}H NMR spectroscopy using dimethyl sulfoxide as internal standard.

Substrate scope

Following the successful catalysis with novel catalysts **1** and **2**, the TH of 27 ketones were examined, under the optimised reaction conditions, using a 1:5:100 ratio of catalyst to KO*t*Bu base to ketone substrates at 80 °C in 2-propanol. The catalytic results are given in **Table 3**.

For the acetophenone substrate, almost quantitative conversions were obtained from both catalysts over a period of 1 h, with similar activity for both catalysts **1** and **2** (entry 1). Catalyst **1** gave excellent yields in the conversion of propiophenone and benzophenone to their corresponding alcohols (99% and 94%, respectively), while catalyst **2** showed much lower activity (7% and 33%, respectively) for the same two substrates (entry 2-3). Given that catalysts **1** and **2** performed similarly with acetophenone substrate, these differences in activity can be attributed to the additional steric effects of the larger substrates, with a likely steric clash between the larger PPh_3 ligand and the larger substrates propiophenone and benzophenone. Another potential explanation for the lower activity of complex **2** is the positive charge on the complex. In related work, Patra and co-workers showed that a neutral Ru(II) catalyst with one PPh_3 group gave higher catalytic activity than a cationic Ru(II) complex bearing two PPh_3 groups, as a result of the lower reduction potential of the neutral compound.[34]

Under catalysis by complex **1**, when acetophenone is substituted by strong electron-donating groups, such as amine and hydroxyl functional groups, the reaction conversion decreases somewhat, with *para*-substitution showing the greatest reduction in reaction conversion, compared to *ortho*- and *meta*-substitutions. For example, 2-aminoacetophenone was hydrogenated to the corresponding alcohol at 52% conversion at 16 h, whereas 39% conversion was observed for 4-aminoacetophenone (entry 4-5). For hydroxyl-substituted acetophenone, there was no difference of catalytic activities between *ortho*- and *meta*-substitutions, converting around 30% conversion within 16 h (entry 6-7), but no alcohol product was obtained when 4-hydroxyacetophenone was used as substrate (entry 8). When catalyst **2** was employed, poor conversions were observed for both amino- and hydroxy-substituted acetophenone (entry 4-8). Substitutions of methoxy and methyl groups at the *para*-position in the reaction catalysed by **1** display moderate and excellent percent conversions up to 78% and 99%, respectively, in 16 h. Interestingly, catalyst **2** showed better catalytic activity for 4-methoxyacetophenone than **1** with 81% conversion after just 1 h. The results with methoxy electron donating groups could imply that the lower conversions observed for amino- and hydroxy- substates arises from the labile protons rather than the electron donation of the substates.

Although the catalytic activities for TH of halide substituted acetophenone seems to fluctuate (entry 11-17), catalyst **1** showed excellent performances over 2-chloroacetophenone (entry 13) and moderate percent conversion for 2-bromoacetophenone, 4-bromoacetophenone and 4-iodoacetophenone (entry 15-17), while low catalytic activities were observed by using catalyst **2**.

For *para*-substituted acetophenone with strong electron-withdrawing groups, moderate catalytic activities of **1** and low activities of **2** were exhibited when 4-acetylbenzonitrile was used as a substrate (entry 18), and no corresponding alcohol product was obtained for 4-nitroacetophenone in TH reactions with either catalyst (entry 19). For aromatic heterocyclic ketones, almost quantitative conversions were observed in 2-acetylpyridine and 2-acetylfuran catalysed by **1**, while catalyst **2** showed poorer performance with these substrates (entry 20-21). Interestingly, 2,2-dimethoxy-2-phenylacetophenone was efficiently hydrogenated by both catalysts, giving similar percent conversions of around 92% in 16 h. Catalysts **1** and **2** showed excellent performances in the reduction of aliphatic and cyclic ketones, with catalyst **2** of particular note, giving almost quantitative conversion within 1 h for each tested substrate, apart from 2-octanone as a substrate.

In summary, catalyst **1** performs better than catalyst **2** for most aromatic ketones and aromatic heterocyclic ketone substrates, while catalyst **2** displays slightly higher catalytic conversion for aliphatic ketones, albeit with both catalysts showing excellent performance against this class of substrate.

Table 3 Substrate scope in catalytic transfer hydrogenation.

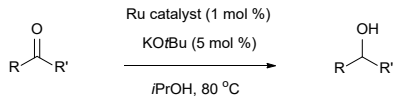

Entry	Substrate	Cat.	Time (h)	Conv. (%)[a]
1	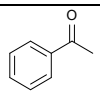	**1**	1	>99 (69[b])
		1	0.5	92
		1	0.16	63
		2	1	>99
2	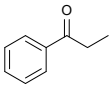	**1**	1	99
		2	1	7
		2	16	99
3	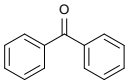	**1**	1	94
		1	16	96
		2	1	33
		2	16	96
4		**1**	1	27
		1	16	52
		2	16	14
5	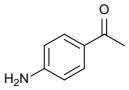	**1**	1	15
		1	16	39
		2	16	3
6		**1**	1	1
		1	16	31
		2	16	3
7	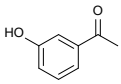	**1**	1	4
		1	16	34
		2	16	0
8	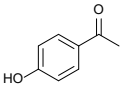	**1**	16	0
		2	16	0
9	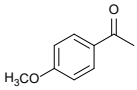	**1**	1	68
		1	16	78
		2	1	81
		2	16	81
10		**1**	1	77
		1	16	99
		2	16	7
11		**1**	16	0
		2	16	0
12	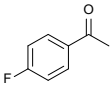	**1**	1	4
		1	16	8
		2	1	7
		2	16	14
13		**1**	1	79
		1	16	>99
		2	16	23
14	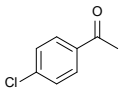	**1**	16	0
		2	16	0

Entry	Substrate	Cat.	Time (h)	Conv. (%)[a]
15		**1**	1	20
		1	16	45
		2	1	4
		2	16	12
16	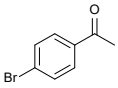	**1**	1	26
		1	16	91
		2	1	14
		2	16	34
17	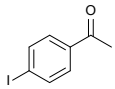	**1**	1	13
		1	16	32
		2	1	5
		2	16	11
18	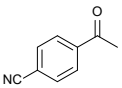	**1**	1	15
		1	16	31
		2	1	6
		2	16	7
19	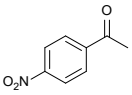	**1**	16	0
		2	16	0
20		**1**	1	56
		1	16	>99
		2	16	0
21		**1**	1	65
		1	16	93
		2	1	4
		2	16	7
22	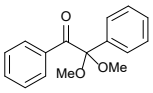	**1**	1	22
		1	16	93
		2	1	63
		2	16	92
23		**1**	1	>99
		2	1	>99
24		**1**	1	78
		1	16	>99
		2	1	>99
25	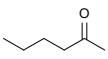	**1**	1	65
		1	16	>99
		2	1	>99
26	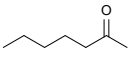	**1**	1	70
		1	16	>99
		2	1	>99
27	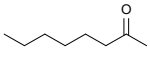	**1**	1	10
		1	16	62
		2	1	>99
28	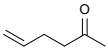	**1**	1	27[c] (7[d])
		1	16	>99[c,d]
		2	1	>99[c] (18[d])

Reaction conditions: substrates (0.5 mmol), KO*t*Bu (0.025 mmol, 5 mol %), Ru catalyst (0.005 mmol, 1 mol %), and 2-propanol (2.5 mL) at 80 °C. [a]Determined by ^{1}H NMR spectroscopy using dimethyl sulfoxide or dimethylformamide as internal standard. [b] yield of isolated products. [c] conversion of ketone, [d] conversion of alkene

As a final compound of interest, we looked at the reaction of 5-hexene-2-one (entry 28). For catalyst **1**, both ketone and alkene were hydrogenated after 16 h. After 1 h, ketone hydrogenation had proceeded to 27%, while alkene hydrogenation was 7%. This illustrates that there is some selectivity to the ketone, but that the catalyst has the ability to hydrogenate both functional groups. For catalyst **2**, hydrogenation of the ketone was complete after 1 h, but alkene hydrogenation had reached only 18% at this time point.

Kinetic data, Eyring analysis and proposed mechanism

Two main mechanisms for ketone transfer hydrogenation catalysed by transition metal complexes have been proposed: (1) an inner-sphere hydride insertion (TI), in which the substrate coordinates directly to metal centre before the hydride transfers from the metal to the *beta* position of the substrate, and (2) an outer-sphere hydride transfer (TO) associated with the delivery of hydride without forming a direct bond between the substrate and metal centre (see Fig S59) .[31,35] To be fully confident of one or other mechanism, a detailed study on transition states and reaction pathways would be required.[36] However, to a simple approximation, hydride transfer in the TI mechanism involves a unimolecular insertion of hydride to substrate, leading to a predicted zero-order depending on substrate concentration. By contrast, TO would show a first-order dependence on substrate, due to a bimolecular hydride transfer reaction between the catalyst and substrate. To propose which mechanism is more likely for catalyst **1**, kinetic analysis was used to determine whether hydride transfer is unimolecular or bimolecular. Kinetic analysis of the reaction of acetophenone with catalyst **1** was carried out using ^{1}H-NMR analysis. As displayed in Fig. 2, the reaction shows a zero-order dependence on acetophenone with a rate constant of 5.69 mM/min. The reaction was repeated at varying starting acetophenone concentrations (Fig S49-51). The results again confirmed a zero-order dependence with respect to acetophenone concentration, with consistent initial rate constants observed between starting acetophenone concentration range 0.2-1.6 M (Figs S52). These results are consistent with an inner-sphere hydride transfer from Ru hydride species to ketone substrate through the primary coordination sphere in the transition state.

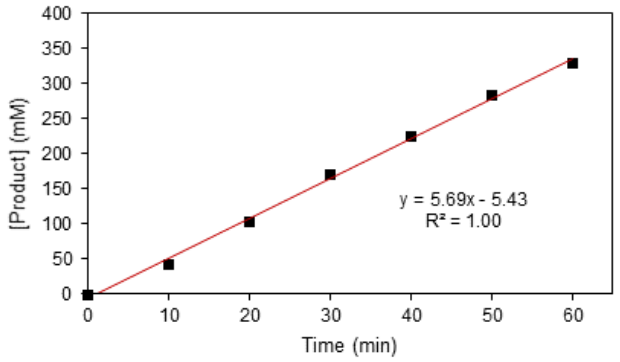

Fig. 2 Kinetic analytical data showing zero order dependence of the reaction on the acetophenone substrate. See supporting information for further data. Conditions: catalyst **1** [Ru] = 2.0 mM, [*i*PrOH] = 13.1 M, [acetophenone]$_0$ = 1.6 M, 80 °C. Determined by ^{1}H-NMR.

To further probe the mechanism, Eyring analysis was conducted, whereby the rate of reaction was measured as a function of temperature. Using ^{1}H NMR analysis at temperatures 50, 60, 70 and 80 °C, a plot of 1/T versus ln (k_i/T) was constructed (Fig. 3 and Fig. S53-57, Table S2). From the data, the following values were calculated: $\Delta H^{\ddagger}$ = 85.3 kJ mol^{-1} and $\Delta S^{\ddagger}$ = 4.2 J mol^{-1} K^{-1}, leading to a calculated free energy of activation ($\Delta G^{\ddagger}$) of 83.8 kJ mol^{-1}.[31,37] A very small positive value of activation entropy is consistent with a unimolecular rate determining step involving inner sphere transfer of hydride to the ketone.[36]

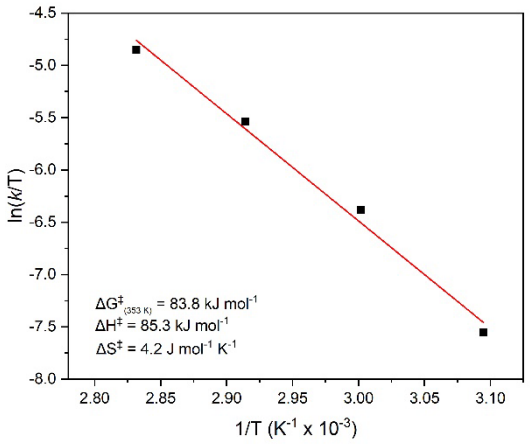

Fig. 3 Eyring plot for Acetophenone TH catalysed by **1** with conditions: Ru:KOtBu:acetophenone = 1:5:100, [Ru] = 2.0 mM, [iPrOH] = 13.1 M, [acetophenone]$_0$ = 0.2 M, temperatures 50, 60, 70, and 80 °C. Determined by ^{1}H-NMR.

By combining the kinetic data and Eyring analysis, an inner sphere mechanism for ketone transfer hydrogenation catalysed by catalyst **1** was proposed, as shown in Fig. 4. The first step of the reaction starts with the introduction of KO*t*Bu and 2-propanol to catalyst **1**, leading to the formation of Ru-alkoxide complex (**A**) through a rapid exchange of chloride ion to alkoxide. After the hydride transfers to Ru centre by β-hydride elimination, the oxidized hydrogen donor is released and the monohydride species (**B**) enters into the catalytic cycle.[38–41] The cleavage of one amine arm provides a catalytic site to allow coordination between the metal centre and oxygen from the ketone substrate (**C**). Inner-sphere hydride transfer from metal to the ketone contributes the rate-determining step, leading to the formation of 16-electron complex (**D**). It is worth noting that the very small magnitude of $\Delta S^{\ddagger}$ (4.2 J mol^{-1} K^{-1}) obtained from Eyring analysis correspond to a unimolecular transition state (**C** → **D**).[42] Protonolysis of the alkoxide with 2-propanol to release substrate generating Ru alkoxide intermediate (**E**) is accelerated in the presence of base,[43] before hydride transfers to provide monohydride Ru complex (**F**), and the catalytic cycle is closed via the final elimination step of acetone.

Conclusions

In conclusion, we have reported a series of novel Ru(II) complexes bearing bipyridine-based ligands (**1-3**) and *N*-heterocyclic carbene-supported pyridine (NCN) ligand (**4-6**). All ligands and complexes were successfully synthesised and characterised by NMR, HRMS, and X-ray crystallography. All complexes were tested as catalysts for transfer hydrogenation of acetophenone in 2-propanol at 80 °C in the presence of catalytic KO*t*Bu base. Activity of the novel compounds was compared to the commercially available Ru-MACHO and Milstein catalysts. Catalysts **1** and **2** displayed excellent catalytic activities in converting acetophenone to its corresponding alcohol and were shown to be active against a panel of 27 ketones. For most aromatic ketones and aromatic heterocyclic ketone substrates, catalyst **1** shows higher activity, while catalyst **2** is more active in the conversion of aliphatic ketones. Finally, Eyring analysis gives an observed zero-order dependence for the acetophenone substrate, leading to a proposed inner-sphere hydride transfer mechanism. Overall, these results give valuable insight into how subtle structural changes at the Ru centre can lead to larger changes in activity in an important transformation in synthetic chemistry.

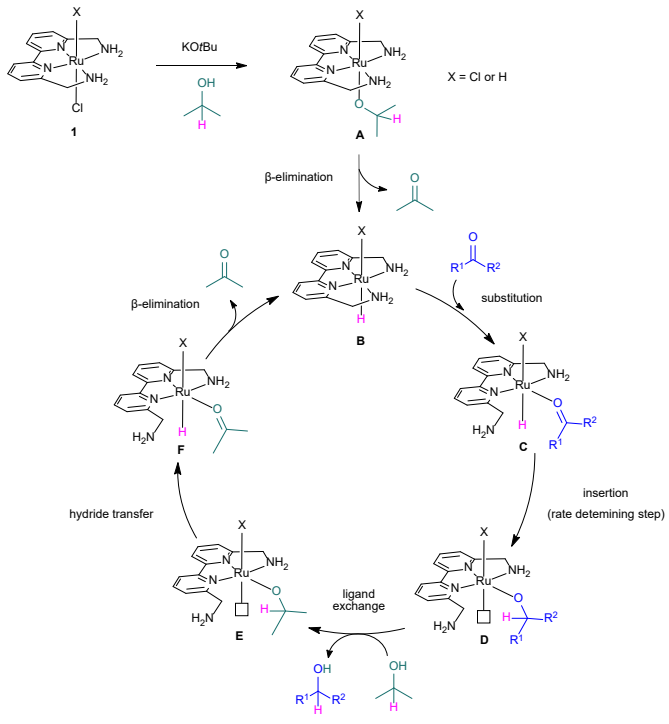

Fig. 4 Proposed catalytic cycle for the acetophenone TH catalysed by **1**.

Experimental section

General considerations

All chemicals were purchased from Sigma Aldrich UK, Fluorochem, Merck, Tokyo chemical industry (TCI), and Fisher UK. Solvents were laboratory grade or dried by the Durham University SPS service. All manipulations of air- and/or moisture-sensitive compounds were carried out under nitrogen atmosphere using the standard Schlenk techniques. Where appropriate, solvents were sparged with nitrogen as a degas method. Thin-layer chromatography was carried out on silica plates (Merck 5554) and visualised under UV (254/365 nm). Preparative column chromatography was carried out using silica (Merck Silica Gel 60, 230400 mesh). ^{1}H and ^{13}C{^{1}H} NMR spectra were recorded on a Varian VNMRS-600 (^{1}H 600.130 MHz and ^{13}C 150.903 MHz) or a Varian VNMRS-700 spectrometer (^{1}H at 699.73 MHz, ^{13}C at 175.95 MHz). Spectra were recorded at 295 K in commercially available deuterated solvents purchased from Sigma Aldrich UK and Goss scientific, and referenced internally to the residual solvent resonances. The multiplicity of each signal is indicated by s (singlet); d (doublet); t (triplet); q (quartet); quin (quintet) or sept (septet). The number of protons (n) for a given resonance signal is indicated by nH. Coupling constants (J) are quoted in Hz and are recorded to the nearest 0.1 Hz. Identical proton coupling constants (J) are averaged in each spectrum and reported to the nearest 0.1 Hz. The coupling constants are determined by analysis using MestreNova software. Spectra were assigned using COSY, NOESY, HSQC and HMBC experiments as necessary. Both electrospray and high-resolution mass spectrometry were performed on a Thermo-Finnigan LTQ FT system using methanol as the carrier solvent. m/z values are reported in Daltons with specific isotopes identified.

Single-crystal X-Ray crystallography

The X-ray single crystal data have been collected using λMoKα radiation (λ = 0.71073 Å) on a Bruker D8Venture (Photon III MM C14 CPAD detector, IμS-III-microsource, focusing mirrors (compounds **2** and **5**); Photon100 CMOS detector, IμS-microsource, focusing mirrors (compounds **L0** and **L1**)) diffractometers equipped with Cryostream (Oxford Cryosystems) open-flow nitrogen cryostats at the temperature 120.0(2) K. All structures were solved by direct method and refined by full-matrix least squares on F^2 for all data using Olex2[44] and SHELXTL[45] software. All non-disordered non-hydrogen atoms were refined in anisotropic approximation; hydrogen atoms in structure **L1** were refined isotropically; hydrogen atoms in all other structures were placed in the calculated positions and refined in riding mode. Disordered atoms in structures **5** and **L1** were refined isotropically. Crystal data and parameters of refinement are listed in Table S1. Crystallographic data for the structures have been deposited with the Cambridge Crystallographic Data Centre as supplementary publications CCDC 2099625-2099628.

Synthetic Procedure

*6,6'-Bis(bromomethyl)-2,2'-bipyridine (**L0**).* Adapting a literature preparation,[29] a mixture of 6,6'-dimethyl-2,2'-bipyridine (1.00 g, 5.42 mmol) and *N*-bromosuccinimide (2.00 g, 11.2 mmol) in $CHCl_3$ (60 ml) was heated to 62 °C for 30 min. Catalytic benzoyl peroxide (400 mg, 1.65 mmol) was added into the solution and the mixture was refluxed at 62 °C for 16 h. The

solvent was removed under reduced pressure. The yellow residue was triturated with MeOH (5 x 10 ml) and the white solid was recrystallized from chloroform to give the product as a white crystalline solid (0.385 g, 21%). ^{1}H NMR (700 MHz, Chloroform-*d*): δ 8.40 (dd, $^3J_{HH}$ = 7.8 Hz, $^4J_{HH}$ = 1.0 Hz, 2H, CH_{py}), 7.84 (t, $^3J_{HH}$ = 7.8 Hz, 2H, CH_{py}), 7.48 (dd, $^3J_{HH}$ = 7.8, $^4J_{HH}$ = 1.0 Hz, 2H, CH_{py}), 4.64 (s, 4H, CH_2).^{13}C{^{1}H} NMR (176 MHz, Chloroform-*d*): δ 156.2 (C_{py}), 155.2 (C_{py}), 138.1 (C_{py}), 123.7 (C_{py}), 120.6 (C_{py}), 33.9 (CH_2). HRMS (ASAP): *m/z* calculated for $[C_{12}H_{11}{}^{79}Br_2N_2]^+$: 340.9289, found: 340.9274.

*6,6'-Bis(aminomethyl)-2,2'-bipyridine (**L1**).* Adapting a literature preparation,[29] 6,6'-bis(bromomethyl)-2,2'-bipyridyl (0.107 g, 0.313 mmol) was dissolved in $CHCl_3$ (5 ml). The solution was heated to 62 °C until the substance dissolved completely. A solution of hexamethylenetetramine (96.7 mg, 0.689 mmol) in $CHCl_3$ (3 ml) was added dropwise. The mixture was refluxed at 62 °C for 4 h, then allowed to cool to room temperature for 24 h. The crude material was isolated by filtration and washed with $CHCl_3$ (5 x 3 ml) and dried under vacuum. The solid was dissolved in water (0.8 ml), EtOH (4 ml) and conc. HCl (1.0 ml) at 70 °C. The solution was left for 24 h at room temperature. A white needle crystalline solid formed and was collected, washed with $CHCl_3$ (3x10 ml) and dried under vacuum to give the HCl salt of the title compound (0.0572 g, 85%). To obtain the neutral compound, the crystalline solid was dissolved in water (5 ml) and 6M NaOH (5 ml). The solution was extracted with CH_2Cl_2 (3 x 10 ml) and $CHCl_3$ (2 x 10 ml). The organic layers were combined, dried under $MgSO_4$ and the solvent was removed under reduced pressure to give a bright yellow solid (0.0426 g, 62%). ^{1}H NMR (599 MHz, Methanol-d_4) δ 8.36 (d, $^3J_{HH}$ = 7.7 Hz, 2H, CH_{py}), 7.89 (t, $^3J_{HH}$ = 7.7 Hz, 2H, CH_{py}), 7.40 (d, $^3J_{HH}$ = 7.7 Hz, 2H, CH_{py}), 4.03 (s, 4H, CH_2). ^{13}C{^{1}H} NMR (176 MHz, Methanol-d_4) δ 160.9 (C_{py}), 156.8 (C_{py}), 138.9 (C_{py}), 122.8 (C_{py}), 120.7 (C_{py}), 47.2 (CH_2). HRMS (ESI): *m/z* calculated for $[C_{12}H_{15}N_4]^+$: 215.1297, found: 215.1296.

*6,6'-bis(dimethylaminomethyl)-2,2'-bipyridine (**L2**).* Adapting a literature preparation,[29] 6,6'-bis(bromomethyl)-2,2'-bipyridyl (0.268 g, 0.784 mmol) was dissolved in ethanol (10 ml). A 40% (w/w) aqueous solution of dimethylamine (4.0 ml, 8.0 mmol) was added dropwise. The mixture was refluxed at 80 °C for 16 h, then allowed to cool to room temperature. The solvent was removed under reduced pressure. To deprotonate the compound, the white residue was dissolved in water (5 ml) and 6M NaOH (5 ml). The solution was extracted with $CHCl_3$ (3 x 10 ml). The organic layers were combined, dried under $MgSO_4$ and the solvent was removed under reduced pressure. The solid was dried under high vacuum to give a bright yellow solid (0.212 g, 100%). ^{1}H NMR (700 MHz, Deuterium Oxide): δ 8.40 (dd, $^3J_{HH}$ = 7.9, $^4J_{HH}$ = 3.3 Hz, 2H, CH_{py}), 8.10 (t, $^3J_{HH}$ = 7.9 Hz, 2H, CH_{py}), 7.61 (dd, $^3J_{HH}$ = 7.9, $^4J_{HH}$ = 3.3 Hz, 2H, CH_{py}), 4.59 (s, 4H, CH_2), 3.03 (s, 12H, CH_3). ^{13}C{^{1}H} NMR (176 MHz, Deuterium Oxide): δ 155.3 (C_{py}), 149.5 (C_{py}), 139.3 (C_{py}), 124.9 (C_{py}), 122.1 (C_{py}), 61.1 (CH_2), 43.0 (CH_3). HRMS (ESI): m/z calculated for $[C_{16}H_{23}N_4]^+$: 271.1923, found: 271.1928.

*1,3-bis(2-methylpyridyl)imidazolium bromide (**L3**).* According to a literature preparation,[30] 2-Bromomethylpyridine (0.446 g, 1.76 mmol), imidazole (61.8 g, 0.907 mmol) and potassium carbonate (0.220 g, 2.61 mmol) were dissolved in methanol (5 mL) and refluxed at 66 °C for 48 h. The mixture was filtered off through celite and washed with methanol (3 x 5 mL). The filtrate was evaporated to give a crude brown oil. This residue was triturated with dichloromethane (2 mL) and tetrahydrofuran (10 mL) and the supernatant was collected, the solvent removed and then the resultant brown oil was dried under vacuum to obtain the title compound. Yield: 0.2461 g, 84%. ^{1}H NMR (599 MHz, Chloroform-*d*): δ 10.95 (s, 1H, CH_{im}), 8.57 – 8.53 (m, 2H, CH_{py}), 7.79 – 7.73 (m, 4H, CH_{py}), 7.54 (d, $^3J_{HH}$ = 1.6 Hz, 2H, CH_{im}), 7.33 – 7.28 (m, 2H, CH_{py}), 5.66 (s, 4H, CH_2). ^{13}C{^{1}H} NMR (151 MHz, Chloroform-*d*): δ 152.2 (C_{im}), 149.9 (C_{py}), 137.9 (C_{py}), 124.2 (C_{py}), 124.1 (C_{py}), 122.2 (C_{im}), 54.2 (CH_2). HRMS (ASAP): *m/z* calculated for $[C_{15}H_{15}N_4]^+$: 251.1297, found: 251.1305.

*Preparation of [Ru(**L1**)Cl$_2$] (**1**).* $[RuCl_2(p\text{-cymene})]_2$ (0.046 g, 0.072 mmol) and 6,6'-Bis(aminomethyl)-2,2'-bipyridine (0.040 g, 0.18 mmol) were dissolved in degassed dry dichloromethane (4 mL) under N_2 atmosphere. The mixture was stirred at room temperature for 1 h to give a deep green suspension. The suspension was added into cold Hexane (20 mL) in dry ice bath to obtain precipitation. The suspension was filtered and the solid was washed with Et_2O (3 x 15 mL) and dried under vacuum to give air-sensitive pure green solid. Yield: 0.0553 g, 99%. ^{1}H NMR (599 MHz, Chloroform-*d*): δ 7.93 (d, $^3J_{HH}$ = 8.0 Hz, 2H, CH_{py}), 7.46 (d, $^3J_{HH}$ = 7.9, 2H, CH_{py}), 7.34 (d, $^3J_{HH}$ = 7.7 Hz, 2H, CH_{py}), 4.70 (t, $^3J_{HH}$ = 6.2 Hz, 4H, CH_2), 4.40 (s, 4H, NH_2). ^{13}C{^{1}H} NMR (151 MHz, Chloroform-*d*): δ 162.1 (C_{py}), 160.6 (C_{py}), 128.6 (C_{py}), 120.9 (C_{py}), 119.0 (C_{py}), 53.0 (CH_2). HRMS (ESI): *m/z* calculated for $[C_{12}H_{14}N_4{}^{35}Cl^{96}Ru]^+$: 344.9983, found: 344.9958. Anal. found (Expected): C 37.09 (37.32); H 3.07 (3.65); N 13.07 (14.51). dec pt >200 °C (capillary, no melting). FTIR: ν_{max} 3227 (br w), 2207 (w), 1595 (s), 767 (s).

*Preparation of [Ru(**L1**)(PPh$_3$)Cl]Cl (**2**).* $[[(C_6H_5)_3P]_3RuCl_2]$ (46.6 mg, 0.0486 mmol) and 6,6'-bis(aminomethyl)-2,2'-bipyridine (**L1**) (10.0 mg, 0.0500 mmol) were dissolved in anhydrous $CHCl_3$ (5 mL) and refluxed at 62 °C for 14 h. The solid was filtered off and washed with $CHCl_3$ (3 x 5 mL). The solid was dissolved in methanol. Undissolved impurities were removed by filtration and the filtrate was evaporated to give a dark brown solid, which was dried under high vacuum to give the title compound. The solid was recrystallized by vapour-diffusion method in methanol and diethyl ether to give a black crystalline solid (0.0251, 81%). ^{1}H NMR (599 MHz, Methanol-d_4): δ 8.15 (d, $^3J_{HH}$ = 8.0 Hz, 2H, CH_{py}), 7.78 (t, $^3J_{HH}$ = 8.0 Hz, 2H, CH_{py}), 7.43 (t, $^3J_{HH}$ = 7.7 Hz, 3H, CH_{phe}), 7.32 (d, $^3J_{HH}$ = 8.0 Hz, 2H, CH_{py}), 7.28 (td, $^3J_{HH}$ = 7.7, $^3J_{HH}$ = 2.1 Hz, 6H, CH_{phe}), 7.04 – 7.01 (m, 6H, CH_{phe}), 4.68 (s, 1H, NH_2), 4.32 – 4.27 (m, 2H, CH_2), 4.09 (s, 1H, NH_2), 3.46 (dd, $^2J_{HH}$ = 17.5, $^3J_{HH}$ = 7.2 Hz, 2H, CH_2). ^{13}C{^{1}H} NMR (151 MHz, Methanol-d_4): δ 162.7 (C_{py}), 157.5 (C_{py}), 133.6 (C_{py}), 132.7 (C_{phe}), 132.6 (C_{phe}), 130.0 (C_{phe}), 128.6 (C_{phe}), 128.5 (C_{phe}), 121.1 (C_{py}), 121.0 (C_{py}), 52.9 (CH_2). ^{31}P NMR (162 MHz, DMSO-d_6): δ 58.5. HRMS (ESI): *m/z* calculated for $[C_{30}H_{29}N_4P^{96}Ru]^{2+}$: 286.0591, found: 286.0566. dec pt >240 °C (capillary, no melting). FTIR: ν_{max} 3114 (br w), 1597 (s), 696 (br).

*Preparation of [Ru(**L2**)Cl$_2$] (**3**).* $[RuCl_2(p\text{-cymene})]_2$ (72.7 mg, 0.118 mmol) and 6,6'-bis(dimethylaminomethyl)-2,2'-

bipyridine (**L2**) (72.6 mg, 0.268 mmol) were dissolved in degassed dry dichloromethane (2 mL) under N_2 atmosphere. The mixture was heated to 50 °C for 16 h to give a deep green suspension. Hexane (100 mL) was added into the solution causing a precipitation to form, which was isolated by decanting. The solid was dissolved in toluene (2 mL) and undissolved impurities were filtered off. Solvent was removed from the filtrate under reduced pressure and the residue dried under vacuum to give a green oil. The complex was purified by flash column chromatography with alumina as the stationary phase and CH_2Cl_2 as the mobile phase to give the title compound (0.0482, 78%). ^{1}H NMR (700 MHz, Chloroform-*d*): δ 7.87 (d, $^3J_{HH}$ = 7.8 Hz, 2H, CH_{py}), 7.46 (t, $^3J_{HH}$ = 7.8 Hz, 2H, CH_{py}), 7.29 (d, $^3J_{HH}$ = 7.8 Hz, 2H, CH_{py}), 4.16 (s, 4H. CH_2), 3.14 (s, 12H, CH_3). ^{13}C{^{1}H} NMR (176 MHz, Chloroform-*d*): δ 162.8 (C_{py}), 161.7 (C_{py}), 129.7 (C_{py}), 120.7 (C_{py}), 119.9 (C_{py}), 71.4 (CH_2), 54.5 (CH_3). HRMS (ESI): *m/z* calculated for $[C_{16}H_{22}N_4{}^{35}Cl^{96}Ru]^+$: 401.0609, found: 401.0629. dec pt >200 °C (capillary, no melting). FTIR: ν_{max} 2883 (br w), 1598 (s), 777 (br).

*Preparation of [RuCp(**L3**)]PF$_6$ (**4**).* 1,3-bis(2-methylpyridyl)imidazolium bromide (**L3**) (83.9 mg, 0.253 mmol) and silver oxide (28.8 mg, 0.123 mmol) were added into EtOH (5 mL) and dichloromethane (5 mL). The mixture was stirred at room temperature for 1.5 h in dark. After adding [CpRu(MeCN)$_3$]PF$_6$ (100 mg, 0.230 mmol), the mixture was heated to 50 °C for 16 h in dark to give a brown suspension. The residue was filtered off and washed with dichloromethane (4 x 1 mL). Undissolved impurities were removed by filtration and the filtrate was evaporated to give a dark brown solid, which was dried under vacuum. The solid was washed with Et_2O (3 x 2 mL) and chloroform (3 x 4 ml) and dried under high vacuum to give the title compound (0.0696, 53.8%). ^{1}H NMR (599 MHz, Acetone-d_6) δ 9.80 (d, $^3J_{HH}$ = 5.6 Hz, 2H, CH_{phe}), 7.88 (t, $^3J_{HH}$ = 7.6 Hz, 2H, CH_{phe}), 7.66 (d, $^3J_{HH}$ = 7.6 Hz, 2H, CH_{phe}), 7.53 (s, 2H, CH_{im}), 7.37 (td, $^3J_{HH}$ = 7.6, $^3J_{HH}$ = 5.6, 2H, CH_{phe}), 5.67 (d, $^2J_{HH}$ = 14.7 Hz, 2H, CH_2), 5.27 (d, $^2J_{HH}$ = 14.7 Hz, 2H, CH_2), 4.49 (s, 5H, Cp). ^{13}C{^{1}H} NMR (176 MHz, Acetone-d_6): δ 158.3 (C_{phe}), 137.5 (C_{phe}), 125.0 (C_{phe}), 123.8 (C_{phe}), 121.3 (C_{im}), 72.4 (Cp), 54.7 (CH_2). HRMS (ESI): *m/z* calculated for $[C_{20}H_{19}N_4{}^{96}Ru]^+$: 411.0686, found: 411.0689. dec pt >210 °C (capillary, no melting) FTIR: ν_{max} 2981 (br w), 1423 (s), 829 (br).

Preparation of [RuCp(**L3**)]PF$_6$ (**5**).* 1,3-bis(2-methylpyridyl)imidazolium bromide (75.8 mg, 0.228 mmol) and silver oxide (27.1 mg, 0.117 mmol) were added into EtOH (5 mL) and dichloromethane (5 mL). The mixture was stirred at room temperature for 1.5 h in dark. After adding [Cp*Ru(MeCN)$_3$]PF$_6$ (99.3 mg, 0.197 mmol), the mixture was heated to 50 °C for 16 h in dark to give a brown suspension. The residue was filtered off and washed with dichloromethane (4 x 1 mL). Undissolved impurities were removed by filtration and the filtrate was evaporated to give a dark brown solid, which was dried under vacuum. The solid was washed with Et_2O (3 x 2 mL) and chloroform (3 x 4 ml) and dried under high vacuum. The solid was recrystallized by slow evaporation in dichloromethane and ethanol (1:1) to give to give a red crystalline solid (0.0746, 60%). ^{1}H NMR (599 MHz, Acetone-d_6) δ 9.38 (d, J = 5.6 Hz, 2H, CH_{phe}), 7.89 (t, J = 7.6 Hz, 2H, CH_{phe}), 7.66 (d, J = 7.7 Hz, 2H, CH_{phe}), 7.49 (s, 2H, CH_{im}), 7.43 (td, J = 7.6, 5.6, 2H, CH_{phe}), 5.63 (d, J = 15.0 Hz, 2H, CH_2), 5.06 (d, J = 15.0 Hz, 2H, CH_2), 1.57 (s, 15H, CH_{Cp*}). ^{13}C{^{1}H} NMR (176 MHz, Acetone-d_6): δ 157.4 (C_{phe}), 137.3 (C_{phe}), 124.9 (C_{phe}), 124.0 (C_{phe}), 121.1 (C_{im}), 82.1 (Cp*), 53.9 (CH_2), 9.27 (C_{Cp*}). HRMS (ESI): *m/z* calculated for $[C_{25}H_{19}N_4Ru]^+$: 481.1468, found: 481.1449. dec pt >210 °C (capillary, no melting) FTIR: ν_{max} 2901 (br w), 1433 (s), 831 (br).

*Preparation of [Ru(p-cy)(**L3**)Cl]PF$_6$ (**6**).* 1,3-bis(2-methylpyridyl)imidazolium bromide (50.0 mg, 0.151 mmol) and silver oxide (17.5 mg, 0.075 mmol) were added into EtOH (5 mL) and dichloromethane (5 mL). The mixture was stirred at room temperature for 1.5 h in dark. After adding [RuCl$_2$(*p*-cymene)]$_2$ (43.5 mg, 0.071 mmol), the mixture was heated to 70 °C for 16 h in dark to give a brown suspension. $AgPF_6$ (38.0 mg, 0.151 mmol) was added into the mixture and stirred for 10 min. The residue was filtered off and washed with dichloromethane (3 x 2 mL). The filtrate was removed solvent by rotary evaporator and dried under vacuum to obtain yellow oil. The solid was washed with Et_2O (3 x 10 mL) and dried under high vacuum to give the title compound (0.0664 g, 90%). ^{1}H NMR (599 MHz, Chloroform-*d*): δ 9.20 (dd, $^3J_{HH}$ = 5.8, $^4J_{HH}$ = 1.6 Hz, 1H, CH_{py}), 8.65 (ddd, $^3J_{HH}$ = 4.8, $^4J_{HH}$ = 1.8, $^5J_{HH}$ = 0.9 Hz, 1H, CH_{py}), 7.84 (td, $^3J_{HH}$ = 7.7, $^4J_{HH}$ = 1.6 Hz, 1H, CH_{py}), 7.77 (td, $^3J_{HH}$ = 7.7, $^4J_{HH}$ = 1.8 Hz, 1H, CH_{py}), 7.62 (d, $^3J_{HH}$ = 7.7 Hz, 1H, CH_{py}), 7.41 (dt, $^3J_{HH}$ = 7.7, $^5J_{HH}$ = 0.9 Hz, 1H, CH_{py}), 7.37 (d, $^3J_{HH}$ = 2.0 Hz, 1H, CH_{im}), 7.36 – 7.34 (m, 1H, CH_{py}), 7.34 – 7.30 (m, 1H, CH_{py}), 7.01 (d, $^3J_{HH}$ = 2.0 Hz, 1H, CH_{im}), 5.79 (dd, $^3J_{HH}$ = 6.1, $^4J_{HH}$ = 1.4 Hz, 1H, CH_{phe}), 5.77 (d, $^2J_{HH}$ = 15.1 Hz, 1H, CH_2), 5.73 (dd, $^3J_{HH}$ = 6.1, $^4J_{HH}$ = 1.4 Hz, 1H, CH_{phe}), 5.49 (dd, $^3J_{HH}$ = 6.2, $^4J_{HH}$ = 1.4 Hz, 1H, CH_{phe}), 5.42 (d, $^2J_{HH}$ = 14.8 Hz, 1H, CH_2), 5.40 (d, $^3J_{HH}$ = 6.2 Hz, 1H, CH_{phe}), 5.31 (d, $^2J_{HH}$ = 15.1 Hz, 1H, CH_2), 5.10 (d, $^2J_{HH}$ = 14.8 Hz, 1H, CH_2), 2.86 (p, $^3J_{HH}$ = 6.9 Hz, CH), 2.15 (s, 3H,CH_3), 1.21 (d, $^3J_{HH}$ = 6.9 Hz, 6H, CH_3). ^{13}C{^{1}H} NMR (176 MHz, Chloroform-*d*): δ 175.2 (C_{im}), 157.6 (C_{py}), 156.4 (C_{py}), 155.3 (C_{py}), 150.0 (C_{py}), 139.5 (C_{py}), 137.5 (C_{py}), 125.7 (C_{py}), 124.5 (C_{py}), 123.6 (C_{py}), 123.3 (C_{im}), 123.0 (C_{py}), 122.5 (C_{im}), 112.7 (C_{phe}), 101.7 (C_{phe}), 88.0 (C_{phe}), 87.3 (C_{phe}), 85.5 (C_{phe}), 83.7 (C_{phe}), 55.5 (CH_2), 54.8 (CH_2), 31.2 (CH), 23.7 (CH_3), 21.2 (CH_3), 18.4 (CH_3). HRMS (ESI): *m/z* calculated for $[C_{25}H_{28}N_4{}^{35}Cl^{96}Ru]^+$: 515.1078, found: 515.1067. mp 115-117 °C (capillary) FTIR: ν_{max} 2924 (br w), 1440 (s), 830 (br).

Typical procedure for transfer hydrogenation of ketones

Ru catalyst (0.005 mmol, 1 mol%) and KO*t*Bu (0.025 mmol, 5 mol%) were added into a 5 mL microwave vial with a magnetic stirring bar. The vial was sealed by aluminium seal with PTFE/silicone septa. After replacing atmosphere with nitrogen gas four times, 2.0 mL of anhydrous 2-propanol was added, and the solution was stirred at 80 °C for 1 h to activate the catalyst. The reaction started when 1M stock solution of ketone in anhydrous 2-propanol (0.5 mL) was added into the vial. The reaction mixture was stirred at the specified temperature. At the specified time, 0.1 mL of the reaction mixture was collected and added into NMR tube, which contained acetone-d_6 (0.5 mL) and 1.28M dimethyl sulfoxide or dimethylformamide in water as internal standard (22 µL). After the reaction was stopped by mixing with water in the internal standard, ^{1}H NMR spectra was recorded at 295 K to calculate percent conversion. For

acetophenone, after the reaction was finished, the mixture was condensed under reduced pressure, and the corresponding alcohol product was isolated by silica gel column chromatography with eluent: or petroleum ether/dichloromethane (1:1). The alcohol products were identified by comparison with the authentic sample through NMR spectroscopy to give the percent yield. The percent conversions were calculated according the formula: $[I_P \times mmol_{Standard}]/[mmol_{substrate}] \times 100\%$, where $[I_P]$ is the integral value of corresponding alcohol per one proton, $mmol_{Standard}$ is a milimole of internal standard per one proton, and $mmol_{substrate}$ is a milimole of substrate in NMR sample as shown in **Fig S43**.

1-Phenylethanol: The compound was obtained as colorless liquid, 69% yield. R_f = 0.3 (petroleum ether/ethyl acetate = 10:1, v/v). ^{1}H NMR (600 MHz, Acetone-d_6): δ 7.38 (d, $^3J_{HH}$ = 7.7 Hz, 2H, CH_{phe}), 7.30 (t, $^3J_{HH}$ = 7.7 Hz, 2H, CH_{phe}), 7.20 (t, $^3J_{HH}$ = 7.3, 1H, CH_{phe}), 4.84 (q, $^3J_{HH}$ = 6.5 Hz, 1H, CH), 4.12 (s, 1H, OH), 1.39 (d, $^3J_{HH}$ = 6.5 Hz, 3H, CH_3). ^{13}C{^{1}H} NMR (151 MHz, Chloroform-*d*): δ 127.9 (C_{phe}), 126.5 (C_{phe}), 125.2 (C_{phe}), 69.0 (CH), 28.9 (CH_3).

Procedure for kinetic analysis

A stock solution of Ru catalyst was prepared by mixing Ru catalyst **1** (11.6 mg, 0.0300 mmol) and KO*t*Bu (16.8 mg, 0.150 mmol) into a 20 mL microwave vial with a magnetic stirring bar. The vial was sealed by aluminium seal with PTFE/silicone septa. After replacing atmosphere with nitrogen gas four times, 12.0 mL of anhydrous 2-propanol was added, and the solution was stirred at 80 °C for 1 h to activate the catalyst. For each measurement, a 2 mL aliquot of this solution was taken into a microwave vials with a magnetic stirring bar reaction. To this vial was added 0.5 mL of specified stock solution of acetophenone in anhydrous 2-propanol (0.5M - 8M) to give final acetophenone concentrations 0.2 M, 0.8 M and 1.6 M. The reaction mixtures were stirred at 80 °C. Every 10 minutes, 0.1 mL of the reaction mixtures were collected and added into NMR tube, which contained acetone-d_6 (0.5 mL) and 1.28M dimethyl sulfoxide in water as internal standard (22 µL). After the reactions were stopped by mixing with water in the internal standard, ^{1}H NMR spectra were recorded at 295 K to calculate percent conversion.

Procedure for Eyring analysis

A stock solution of Ru catalyst was prepared by mixing Ru catalyst **1** (9.7 mg, 0.025 mmol) and KO*t*Bu (14.0 mg, 0.125 mmol) into a 20 mL microwave vial with a magnetic stirring bar. The vial was sealed by aluminium seal with PTFE/silicone septa. After replacing atmosphere with nitrogen gas four times, 10.0 mL of anhydrous 2-propanol was added, and the solution was stirred at 80 °C for 1 h to activate the catalyst. 8 mL of this solution was divided into four microwave vials with a magnetic stirring bar reaction. To each vial was added 0.5 mL of 1M stock solution of acetophenone in anhydrous 2-propanol. The reaction mixtures were stirred at 50, 60, 70 and 80 °C. Every 5 minutes, 0.1 mL of the reaction mixtures were collected and added into NMR tube, which contained acetone-d_6 (0.5 mL) and 1.28M dimethyl sulfoxide in water as internal standard (22 µL). After the reactions were stopped by mixing with water in the internal standard, ^{1}H NMR spectra were recorded at 295 K to calculate percent conversion.

Conflicts of interest

There are no conflicts to declare.

Acknowledgements

We are greatly appreciated the Thailand Development and Promotion of Science and Technology Talents Project (DPST) and RSC Research Fund grant (R19-8838) for financial support, and the Department of Chemistry, Durham University for supporting facilities of this research.

Notes and references

1 D. Wang and D. Astruc, *Chem. Rev.*, 2015, **115**, 6621–6686.
2 A. A. Mikhailine and R. H. Morris, *Inorg. Chem.*, 2010, **49**, 11039–11044.
3 W. Zuo, A. J. Lough, Y. F. Li and R. H. Morris, *Science (80-.).*, 2013, **342**, 1080–1083.
4 Z. Strassberger, M. Mooijman, E. Ruijter, A. H. Alberts, C. De Graaff, R. V. A. Orru and G. Rothenberg, *Appl. Organomet. Chem.*, 2010, **24**, 142–146.
5 Y. Cheng, X. Y. Lu, H. J. Xu, Y. Z. Li, X. T. Chen and Z. L. Xue, *Inorganica Chim. Acta*, 2010, **363**, 430–437.
6 W. Baratta, M. Ballico, A. Del Zotto, K. Siega, S. Magnolia and P. Rigo, *Chem. - A Eur. J.*, 2008, **14**, 2557–2563.
7 T. Dombray, C. Helleu, C. Darcel and J. B. Sortais, *Adv. Synth. Catal.*, 2013, **355**, 3358–3362.
8 R. V. Jagadeesh, D. Banerjee, P. B. Arockiam, H. Junge, K. Junge, M. M. Pohl, J. Radnik, A. Brückner and M. Beller, *Green Chem.*, 2015, **17**, 898–902.
9 M. Coll, O. Pàmies, H. Adolfsson and M. Diéguez, *ChemCatChem*, 2013, **5**, 3821–3828.
10 M. V. Jiménez, J. Fernández-Tornos, J. J. Pérez-Torrente, F. J. Modrego, P. García-Orduña and L. A. Oro, *Organometallics*, 2015, **34**, 926–940.
11 R. Zhong, Y. N. Wang, X. Q. Guo, Z. X. Chen and X. F. Hou, *Chem. - A Eur. J.*, 2011, **17**, 11041–11051.
12 S. Warsink, I. H. Chang, J. J. Weigand, P. Hauwert, J. T. Chen and C. J. Elsevier, *Organometallics*, 2010, **29**, 4555–4561.
13 M. Yan, T. Jin, Y. Ishikawa, T. Minato, T. Fujita, L. Y. Chen, M. Bao, N. Asao, M. W. Chen and Y. Yamamoto, *J. Am. Chem. Soc.*, 2012, **134**, 17536–17542.
14 R. Ghosh, N. C. Jana, S. Panda and B. Bagh, *ACS Sustain. Chem. Eng.*, 2021, **9**, 4903–4914.
15 J. M. Botubol-Ares, S. Cordón-Ouahhabi, Z. Moutaoukil, I. G. Collado, M. Jiménez-Tenorio, M. C. Puerta and P. Valerga, *Organometallics*, 2021, **40**, 792–803.
16 R. Noyori and S. Hashiguchi, *Acc. Chem. Res.*, 1997, **30**, 97–102.
17 O. Dayan, S. Dayan, I. Kani and B. Çetinkaya, *Appl.*

Organomet. Chem., 2012, **26**, 663–670.
18 I. Nieto, M. S. Livings, J. B. Sacci, L. E. Reuther, M. Zeller and E. T. Papish, *Organometallics*, 2011, **30**, 6339–6342.
19 T. Miura, M. Naruto, K. Toda, T. Shimomura and S. Saito, *Sci. Rep.*, 2017, **7**, 1–10.
20 P. A. Dub and J. C. Gordon, *ACS Catal.*, 2017, **7**, 6635–6655.
21 O. Ogata, Y. Nakayama, H. Nara, M. Fujiwhara and Y. Kayaki, *Org. Lett.*, 2016, **18**, 3894–3897.
22 M. N. Hopkinson, C. Richter, M. Schedler and F. Glorius, *Nature*, 2014, **510**, 485–496.
23 D. A. Hey, R. M. Reich, W. Baratta and F. E. Kühn, *Coord. Chem. Rev.*, 2018, **374**, 114–132.
24 H. V. Huynh, *Chem. Rev.*, 2018, **118**, 9457–9492.
25 I. Ödemir, S. Yaşar and B. Çetinkaya, *Transit. Met. Chem.*, 2005, **30**, 831–835.
26 M. Yiğit, B. Yiğit, I. Özdemir, E. Çetinkaya and B. Çetinkaya, *Appl. Organomet. Chem.*, 2006, **20**, 322–327.
27 V. Dragutan, I. Dragutan, L. Delaude and A. Demonceau, *Coord. Chem. Rev.*, 2007, **251**, 765–794.
28 F. Zeng and Z. Yu, *Organometallics*, 2008, **27**, 6025–6028.
29 Z. Wang, J. Reibenspies, R. J. Motekaitis and A. E. Martell, *J. Chem. Soc. Dalt. Trans.*, 1995, 1511–1518.
30 D. J. O'Hearn and R. D. Singer, *Organometallics*, 2017, **36**, 3175–3177.
31 C. M. Moore, B. Bark and N. K. Szymczak, *ACS Catal.*, 2016, **6**, 1981–1990.
32 J. Shi, B. Hu, X. Chen, S. Shang, D. Deng, Y. Sun, W. Shi, X. Yang and D. Chen, *ACS Omega*, 2017, **2**, 3406–3416.
33 L. Wang and T. Liu, *Tetrahedron Lett.*, 2019, **60**, 150993.
34 A. Maity, A. Sil and S. K. Patra, *Eur. J. Inorg. Chem.*, 2018, **2018**, 4063–4073.
35 S. E. Clapham, A. Hadzovic and R. H. Morris, *Coord. Chem. Rev.*, 2004, **248**, 2201–2237.
36 S. Kozuch and S. Shaik, *Acc. Chem. Res.*, 2010, **44**, 101–110.
37 P. M. Morse, M. D. Spencer, S. R. Wilson and G. S. Girolami, *Organometallics*, 1994, **13**, 1646–1655.
38 E. Baráth, *Catalysts*, 2018, 8, 671.
39 O. Pàmies and J. E. Bäckvall, *Chem. - A Eur. J.*, 2001, **7**, 5052–5058.
40 B. Paul, K. Chakrabarti and S. Kundu, *Dalt. Trans.*, 2016, **45**, 11162–11171.
41 K. Li, J.-L. Niu, M.-Z. Yang, Z. Li, L.-Y. Wu, X.-Q. Hao and M.-P. Song, *Organometallics*, 2015, **34**, 1170–1176.
42 J. F. Hartwig, *Organotransition Metal Chemistry*, University Science Books, Mill Valley, CA, 2010.
43 W. Du, L. Wang, P. Wu and Z. Yu, *Chem. - A Eur. J.*, 2012, **18**, 11550–11554.
44 O. V Dolomanov, L. J. Bourhis, R. J. Gildea, J. A. K. Howard and H. Puschmann, *J. Appl. Crystallogr.*, 2009, **42**, 339–341.
45 G. M. Sheldrick, *Acta Crystallogr. Sect. A*, 2008, **64**, 112–122.